Crystal electric field excitations in the cerium compound $CeRh_3B_2$ studied by inelastic neutron scattering

2007 J. Phys.: Condens. Matter 19 506210

(http://iopscience.iop.org/0953-8984/19/50/506210)

IOP PUBLISHING JOURNAL OF PHYSICS: CONDENSED MATTER

J. Phys.: Condens. Matter **19** (2007) 506210 (13pp) doi:10.1088/0953-8984/19/50/506210

Crystal electric field excitations in the cerium compound $CeRh_3B_2$ studied by inelastic neutron scattering

F Givord[1,5,6], J-X Boucherle[1,6,7], A P Murani[2], R Bewley[3], R-M Galéra[4] and P Lejay[4]

[1] CEA-Grenoble, DSM/DRFMC/SPSMS/MDN, 38054 Grenoble Cedex 9, France
[2] Institut Laue Langevin, BP156, 38042 Grenoble Cedex 9, France
[3] ISIS, Rutherford Appleton Laboratory, Chilton, Didcot, Oxon OX11 0QX, UK
[4] Institut Néel, CNRS, BP166, 38042 Grenoble Cedex 9, France

E-mail: francoise.givord@cea.fr

Received 24 August 2007, in final form 5 October 2007
Published 19 November 2007
Online at stacks.iop.org/JPhysCM/19/506210

Abstract

We have performed inelastic neutron scattering (INS) experiments on $CeRh_3B_2$ at various temperatures to obtain direct information on the crystal electric field (CEF) in this compound, which exhibits some very peculiar magnetic properties for a Ce system: it is ferromagnetic with an unusually high Curie temperature (115 K), which contrasts with a strongly reduced and anisotropic magnetization (0.4 μ_B/fu within the *c*-plane of the hexagonal structure). Measurements with high incident energies show only one well defined magnetic excitation around 150 meV, its exact position varying with the temperature. These results, combined with our previous data of magnetization and magnetic form factor, have permitted us to determine the CEF energy level scheme taking into account the two J multiplets of the Ce^{3+} ion. Information on the ground state (quasielastic contribution and ground state moment) has also been obtained by experiments at low incident energies in the paramagnetic state.

(Some figures in this article are in colour only in the electronic version)

1. Introduction

The $CeRh_3B_2$ intermetallic compound, which crystallizes in the hexagonal $CeCo_3B_2$-type structure, is a very interesting compound with exceptional magnetic properties. It is ferromagnetic up to $T_C = 115$ K [1] and its magnetic properties are highly anisotropic. This

[5] Author to whom any correspondence should be addressed.
[6] CNRS staff.
[7] Present address: dr11, CNRS, BP166, 38042 Grenoble Cedex 9, France.

Curie temperature is by far the highest magnetic ordering temperature ever found in Ce-based intermetallic compounds with non-magnetic partners. The easy magnetization is within the $\boldsymbol{c}$-plane [2], and despite the huge value of T_C the spontaneous magnetization at low temperature is very small, about 0.4 μ_B/fu, a value which is strongly reduced compared to the cerium free ion value (2.14 μ_B). The magnetization along the hard $\boldsymbol{c}$-axis is about five times less than in the $\boldsymbol{c}$-plane. The paramagnetic susceptibility is also quite anisotropic and does not follow the Curie–Weiss law until above 600 K [3]. Magnetization curves measured with fields applied along easy and hard directions, at various temperatures in the ferromagnetic and the paramagnetic states, have been reported and calculated in a recent paper [4].

These anisotropic properties must be related to the large difference between the $\boldsymbol{a}$ and $\boldsymbol{c}$ lattice constants, that is between the Ce–Ce distances along these two directions. This feature, characteristic of the RRh_3B_2 crystal structure, is even further enhanced in $CeRh_3B_2$, with $\boldsymbol{a} = 5.48$ Å and $\boldsymbol{c} = 3.09$ Å at room temperature, and $\boldsymbol{c}$ remaining smaller than in $PrRh_3B_2$ at all temperatures. Moreover, a quite abnormal thermal variation of the $CeRh_3B_2$ lattice parameters has been reported [5]: between 300 and 100 K, the $\boldsymbol{a}$ lattice parameter drastically increases while the decrease of $\boldsymbol{c}$ becomes more pronounced, thus intensifying the difference between $\boldsymbol{c}$ and $\boldsymbol{a}$. Along this $\boldsymbol{c}$-direction, the Ce atoms thus form chains with very short Ce–Ce distances (3.09 Å), even smaller than in α-Ce (3.41 Å). Such short Ce–Ce distances can lead to strong hybridization between the Ce 4f, Ce 5d and conduction electrons and to strong crystal electric field (CEF) effects [6, 7].

A polarized neutron diffraction study [8] has shown that the magnetic properties of $CeRh_3B_2$ arise from a localized Ce 4f moment, together with, in the ferromagnetic state, an anisotropic diffuse magnetization between the Ce atoms along the $\boldsymbol{c}$-chains. The deduced Ce magnetic form factor above $\sin\theta/\lambda = 0.25$ Å^{-1} corresponds to the 4f contribution only and shows a strong anisotropy, which is a signature of the CEF effects. Classical calculations of the Ce 4f form factor within the Ce ground multiplet $J = 5/2$ did not fit this measured anisotropy very well, and a much better agreement was obtained by calculations taking also into account the excited $J' = 7/2$ multiplet [9]. These two multiplet calculations of the 4f moment, together with a conduction electron polarization, were also used in the paper cited above [4] to calculate the magnetization curves.

The knowledge of the CEF parameters is thus essential for obtaining the Ce wavefunctions and calculating the 4f magnetizations and magnetic form factor. Expecting large CEF effects, inelastic neutron scattering (INS) measurements with high incident energies were undertaken to determine the CEF splitting. Because of the anomaly in the temperature dependence of the lattice parameters, spectra were collected at several temperatures in the paramagnetic state, as well as at low temperature in the ferromagnetic state, to link the results with the magnetic form factor data. Complementary experiments at low incident energies have also been performed, especially in the paramagnetic phase, to provide information on the ground state: associated quasielastic response, intrinsic moment and possible changes above T_C.

2. Experimental details and results

2.1. Experimental details

Spectra with high incident energies were collected on the time-of-flight spectrometer HET at the pulsed source ISIS (Didcot, UK), with different incident energies E_i between 150 and 900 meV. The resolution of the device, given by the width of the elastic peak, is progressively broader with increasing incident energy (see the half-widths at half-maximum (HWHMs) in table 1). Experiments with low incident energies were performed in the paramagnetic

Table 1. Sixth order CEF parameter $A_6^0\langle r^6\rangle$ at $T = 18$, 150 and 300 K and HWHM values of the elastic peak σ_0, of the quasielastic peak σ_{quasi}, of the CEF peak σ_{CEF} used in the calculations as well as of the measured peaks σ_{peak}, at the different incident energies E_{i}.

T (K)	$A_6^0\langle r^6\rangle$ (K)	E_{i} (meV)	σ_0 (meV)	σ_{quasi} (meV)	σ_{CEF} (meV)	σ_{peak} (meV)
18	−350	450	23	—	38	44
150	−311	150	5	2.3	—	—
		300	9		38	39
		450	23		38	44
		900	40		38	55
300	−218	450	23	5.0	38	44

state at I.L.L. (Grenoble, France): (i) the cold neutron time-of-flight spectrometer IN6 with a very good energy resolution (incident energy 3.1 meV) has permitted us to determine the quasielastic scattering contribution; (ii) the integrated magnetic contribution within the ground state (i.e. that represented by the quasielastic scattering) was determined by the xyz polarization analysis method provided by D7 using neutrons of incident energy 9 meV.

For all experiments, scattering angles range from low angles (5°–10°) to high angles (130°–150°), which allows one to follow the angular dependence of the magnetic and phonon scattering. As we are searching for magnetic phenomena, all the spectra presented in this paper are those obtained at low scattering angles, unless otherwise specified. Spectra for vanadium and cadmium were also measured in order to perform calibrations and the appropriate corrections of the data.

In addition to $CeRh_3B_2$, the isostructural non-magnetic $LaRh_3B_2$ compound has also been measured in order to obtain information about the phonons. For both compounds, the samples were high quality powders of mass around 20 g and the same samples were used for all the experiments reported here. After preparing and annealing, they were kept stocked under vacuum, throughout over the period of the experiments, to avoid hydrogen contamination. As boron has a very high absorption cross section for neutrons, the isotopically enriched ^{11}B was used in the preparation of the samples. However, there are still some absorption effects due to the rhodium. To minimize this absorption, the powder was put into a concentric sample holder for the low energy experiments (D7 and IN6). The optimum thickness was chosen to be that given by $1/e$ transmission at the incident wavelength employed. For the high energy experiments (HET), powders were wrapped in aluminum foils to obtain packages of about $40 \times 40 \times 3$ mm^3.

2.2. Crystal electric field splitting

Because of the expected large CEF splitting, the spectra were first collected at $E_{\text{i}} = 450$ meV. Figure 1 shows the raw data obtained in the paramagnetic state at $T = 150$ K on $CeRh_3B_2$ and at 15 K on $LaRh_3B_2$ for small scattering angles (left part) and for high scattering angles (right part). For the low scattering angles, one small but relatively wide peak is observed around 150 meV in the $CeRh_3B_2$ spectrum, a peak which is not present for the $LaRh_3B_2$ compound. This $CeRh_3B_2$ peak has almost disappeared at high scattering angles, which indicates its magnetic origin. The Ce spectrum has been corrected for the lattice contribution by subtracting the normalized La spectrum and the corrected intensities are reported in figure 2. Besides the main peak at 150 meV, no well defined inelastic peak is noticeable, except a very small and narrow one around 50 meV and a long tail of scattered intensity above 200 meV.

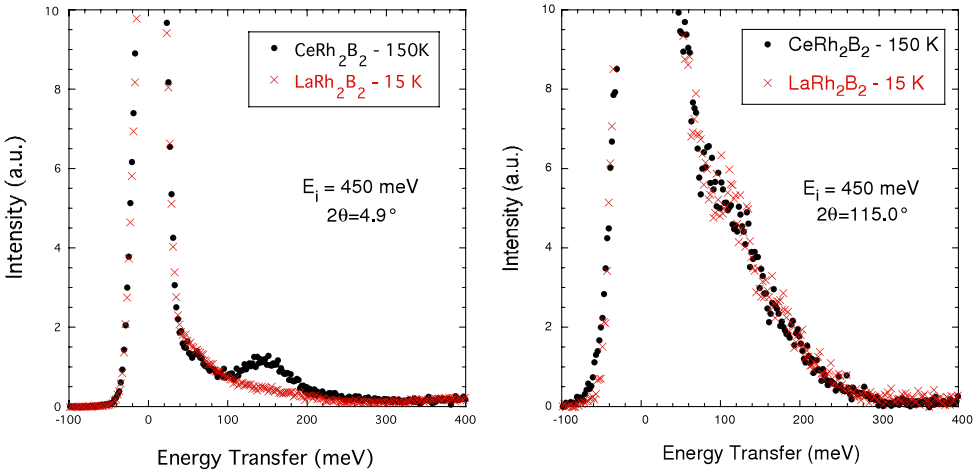

Figure 1. Spectral response obtained with an incident energy $E_i = 450$ meV on $CeRh_3B_2$ at $T = 150$ K and on $LaRh_3B_2$ at $T = 15$ K. The left part corresponds to low scattering angle data ($2\theta = 4.9°$) and the right part to high angle data ($2\theta = 115.0°$).

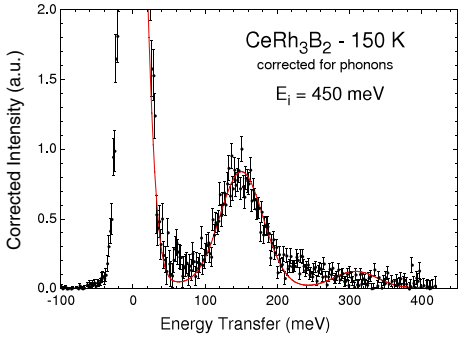

Figure 2. Spectral response corrected for phonons of $CeRh_3B_2$ at $T = 150$ K, with incident energy $E_i = 450$ meV at scattering angle $2\theta = 4.9°$. The full line is the response calculated as explained in the text.

INS measurements at $E_i = 450$ meV were also performed at other temperatures: at 300 K, far above the ordering temperature, and at low temperature (18 K) to allow comparison with the magnetic form factor which, because of the very small Ce magnetic moment, is much more accurate in the ferromagnetic state. The results (top part of figure 3) reveal a significant change in the position of the observed peak, from 132 meV at 300 K to 167 meV at 18 K. Its intensity and width are temperature independent. The latter seems quite large: it is about twice as large as the elastic peak. As the resolution is rather poor at this high energy (HWHM = 23 meV; see table 1), the peak was also measured with an incident energy E_i =300 meV for which the resolution is much improved (HWHM = 9 meV). The observed width remains about the same at $E_i = 300$ meV as at $E_i = 450$ meV (bottom part of figure 3). So, the large width of the CEF peak is not due to the resolution of the device but is an intrinsic property of the $CeRh_3B_2$ compound. HWHM has been evaluated to be 38 meV.

In order to look for other significant information concerning the CEF splitting, an experiment with a higher incident energy $E_i = 900$ meV was performed at 150 K. As can

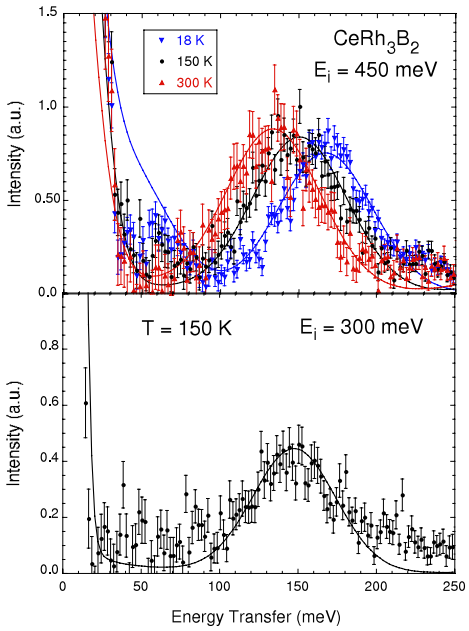

Figure 3. CEF excitation around 150 meV observed at scattering angle $2\theta = 4.9°$. Top part: with the incident energy $E_i = 450$ meV, at three temperatures 300, 150 and 18 K. Bottom part: with an incident energy $E_i = 300$ meV, reported at the same energy transfer scale. The full lines are calculated as explained in the text.

be seen in figure 4, the previously detected peak at 150 meV is still well defined, but no other definite peak is found at higher energy transfer, either in the raw data (top part of figure 4), or in the spectra corrected for phonons (bottom part of figure 4). No measurements on the La compound were performed at this energy, so the intensities at high scattering angles have been used for the phonon corrections instead.

Finally, spectra at several temperatures were collected at $E_i = 150$ meV to study the small peak around 50 meV. This peak is also visible in the $LaRh_3B_2$ spectrum (top of figure 5), which indicates a phonon contribution around this energy transfer. However, for the $CeRh_3B_2$ compound, its intensity at the same temperature (15 K) is a little higher, and, furthermore, it appears to have decreased when the temperature is increased to 150 K, which is not expected for a phonon process. Its persistence up to $T = 300$ K means that this peak is not totally associated with the magnetic ordering. Its decreasing intensity on heating, together with its constant position in energy, indicate that, if it is a CEF peak, it is not similar to the one observed around 150 meV.

Thus, only one well defined magnetic excitation that can be undoubtedly attributed to a CEF transition has been identified with an energy transfer around 150 meV, its exact value depending on the temperature.

2.3. Ground state

The measurements with polarized neutrons on spectrometer D7 of the integrated cross section of the ground state were performed at 300 K and at 120 K, just above the Curie temperature of 115 K. The onset of the ferromagnetic ordering is identified quite clearly from the variation of the flipping ratio with temperature. Figure 6 reports the marked neutron beam

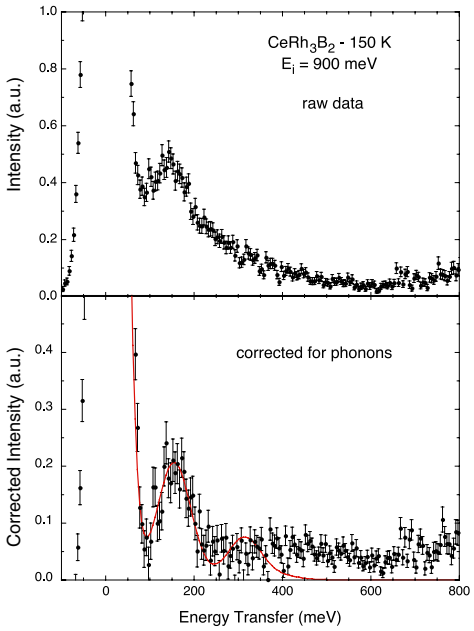

Figure 4. Spectral response obtained at scattering angle $2\theta = 4.9°$, with an incident energy $E_i = 900$ meV. Top part: raw data. Bottom part: data corrected for phonons. The full line is the response calculated as explained in the text.

depolarization with decreasing temperature below the ordering temperature, in a manner resembling, qualitatively, an inverted magnetization curve. The observed scattering cross section as a function of κ ($\kappa = |\boldsymbol{k} - \boldsymbol{k}'|$) at the two temperatures (within an energy window of around $\pm$ 10 meV, corresponding to the incident neutron wavelength of 3.1 Å) is shown in figure 7. The cross section value at $\kappa = 0$ was determined by taking a single average over all the data points. This is justified by the fact that the Ce^{3+} form factor is almost flat over the narrow, low-κ range of the measurements, as indicated by the solid line through the points. Despite the relatively poor precision due to the weakness of the measured signal, we find that the resulting average cross section is about the same at both temperatures. It corresponds to a moment of $0.84 \pm 0.80\ \mu_B$, a value in good agreement with our determination, from magnetization data, of the magnetic moments at 300 K [4]: 0.95 μ_B in the $\boldsymbol{c}$-plane and 0.67 μ_B along the $\boldsymbol{c}$-direction, that is, a mean value of 0.86 μ_B for a powder sample.

The experiments on the IN6 spectrometer with a very good energy resolution (70 μeV) were performed at two temperatures in the paramagnetic phase ($T = 150$ and 300 K), and in the ferromagnetic phase ($T = 10$ K). $LaRh_3B_2$ was also measured at the same temperatures as a reference for non-magnetic contributions. The La spectra were normalized to the Ce ones, taking into account the different masses and transmission factors of the two samples. Figure 8 shows the corrected difference spectra (Ce–La) at the three temperatures. The difference spectrum in the ferromagnetic state ($T = 10$ K) is flat and negligibly small. In contrast, the difference spectra in the paramagnetic state ($T = 150$ and 300 K) show the presence of a well defined quasielastic contribution. The HWHM of this quasielastic peak, fitted by a Lorentzian function centered at the origin, is $\sigma_{quasi} = 2.32 \pm 0.35$ meV at 150 K and $\sigma_{quasi} = 5.02 \pm 0.94$ meV at 300 K. Note that these values are polycrystalline averages and should be very different along the $\boldsymbol{a}$- and $\boldsymbol{c}$-directions.

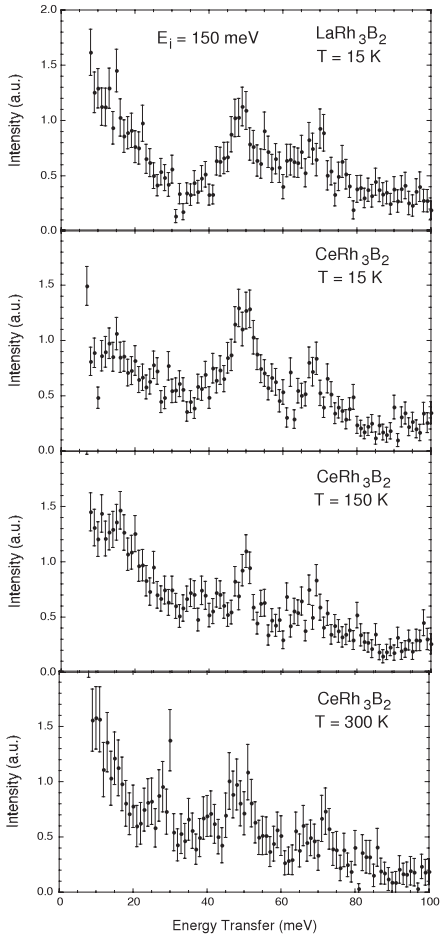

Figure 5. Spectral response obtained at scattering angle $2\theta = 4.9°$, with an incident energy $E_i = 150$ meV on $LaRh_3B_2$ at $T = 15$ K and on $CeRh_3B_2$ at $T = 15$, 150 and 300 K.

3. Discussion

The peak at 150 meV must correspond to a transition from the fundamental doublet to another doublet of the Ce multiplet decomposition by the CEF. As the involved energy is quite large compared with the separation of ≈ 280 meV [10] between the two Ce^{3+} multiplets $J = 5/2$ and $J' = 7/2$, both have to be considered in the calculations. There are then seven doublets, but we have observed only one well defined transition between them. More information on the CEF scheme can be obtained from other CEF sensitive properties measured on a single crystal such as magnetizations along easy and hard directions and the Ce 4f magnetic form factor. These data are directly related to the wavefunction of the thermally occupied energy levels; in particular, the anisotropy of the magnetic form factor is a very good signature of the CEF effects [11]. In the case of $CeRh_3B_2$, the Ce magnetic moment being very small, the data obtained at low temperatures in the ferromagnetic state present a much better accuracy. The CEF parameters have therefore been refined to fit these various types of data and thus fulfill together the following three conditions: (i) a wavefunction in agreement with the anisotropy

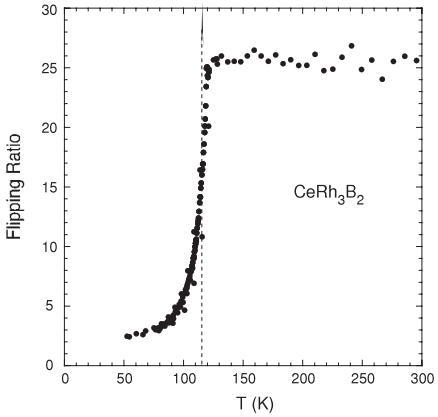

Figure 6. Flipping ratio of $CeRh_3B_2$ measured with polarized neutrons on D7 as a function of temperature.

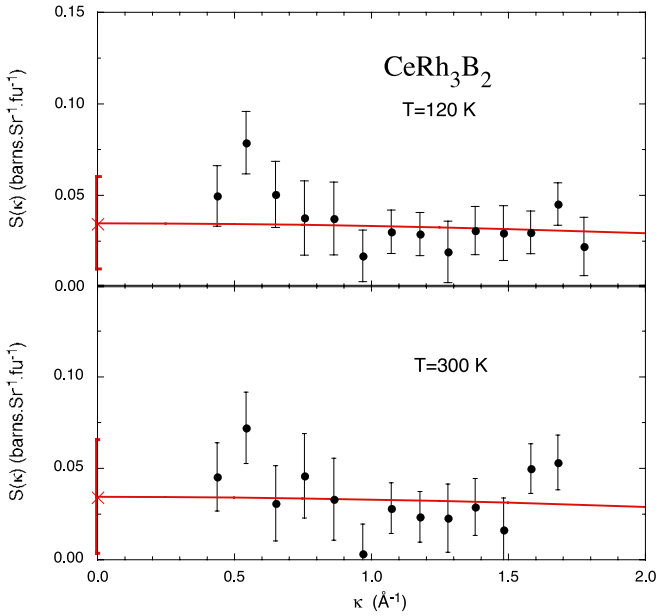

Figure 7. Scattering cross sections of $CeRh_3B_2$ measured on D7 at 120 and 300 K, as a function of κ. At both temperatures, the full line is the Ce^{3+} form factor.

of the magnetic form factor, (ii) the easy magnetization direction in the basal plane of the hexagonal structure and (iii) a CEF peak at an energy transfer around 150 meV.

The model is that previously described [4, 9], in which the Ce energy states are obtained by diagonalizing the following Hamiltonian:

$$\mathcal{H} = \lambda \boldsymbol{L}\cdot\boldsymbol{S} + \mathcal{H}_{\mathrm{CF}} - 2J_{ff}\langle S\rangle \boldsymbol{S} + \mu_{\mathrm{B}}\boldsymbol{H}\cdot(\boldsymbol{L}+2\boldsymbol{S}) + 2\mu_{\mathrm{B}}K_{\mathrm{pol}}\boldsymbol{H}\cdot\boldsymbol{S}, \qquad (1)$$

where $\boldsymbol{L}$ and $\boldsymbol{S}$ are respectively the orbital and spin operators, μ_{B} the Bohr magneton and $\boldsymbol{H}$ the external field. For cerium, the value of the spin–orbit coupling coefficient λ was taken as 930 K ($\lambda = \Delta/J'$ with $\Delta = 280$ meV or 3250 K). J_{ff} is the exchange interaction coefficient and K_{pol} a conduction electron polarization coefficient operating in magnetization calculations.

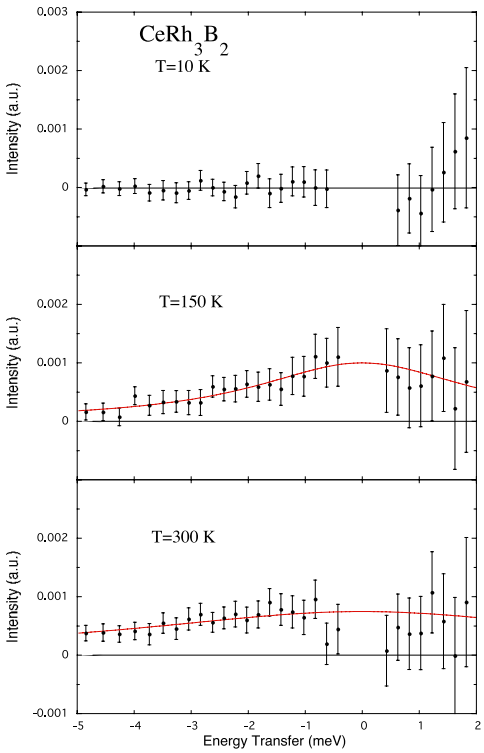

Figure 8. Difference between $CeRh_3B_2$ and $LaRh_3B_2$ spectra measured on IN6 at low scattering angles at T =10, 150 and 300 K. Full lines at 150 and 300 K are fitted Lorentzians (see the text).

The CEF Hamiltonian $\mathcal{H}_{\rm CF}$ for systems including several multiplets can be expressed [12] in a way similar to the Stevens formalism, using the tensor operator techniques of Racah [13]:

$$\mathcal{H}_{\rm CF} = \sum_{k,q} N_k^q A_k^q \langle r^k \rangle U_k^q \tag{2}$$

the N_k^q and U_k^q terms are tabulated [14, 9] and the $A_k^q \langle r^k \rangle$ are the CEF parameters. For hexagonal symmetry, there are four independent ones: $A_2^0\langle r^2\rangle$, $A_4^0\langle r^4\rangle$, $A_6^0\langle r^6\rangle$ and $A_6^6\langle r^6\rangle$. The sixth order terms, which are null for Ce in calculations within the ground multiplet $J = 5/2$ only, are present because of the contribution of the $J' = 7/2$ multiplet.

Knowing the energy levels and their associated wavefunctions, the magnetic spectral function for transitions between levels m and n separated by ΔE_{nm} is proportional to

$$S(\kappa,\omega) \propto F^2(\kappa, J, J') \frac{\hbar\omega}{1 - \mathrm{e}^{\frac{-\hbar\omega}{kT}}} \sum_m \frac{1 - \mathrm{e}^{\frac{-\Delta E_{nm}}{kT}}}{\Delta E_{nm}} p_m \left| \langle n | (\boldsymbol{L} + 2\boldsymbol{S})_\perp | m \rangle \right|^2 \mathcal{F}_{nm}(\kappa,\omega), \tag{3}$$

where $F^2(\kappa, J, J')$ is related to the inelastic structure factor $\mathcal{G}(\kappa, J, J')$ for the multiplets J and J' (see its calculation in the appendix), p_m is the probability of occupation of level m given by the Maxwell–Boltzmann statistic and $\mathcal{F}_{nm}(\kappa,\omega)$ is a spectral function which can be a Lorentzian or a Gaussian function.

The total calculated spectrum is the sum of the following contributions: the elastic peak arising from incoherent scattering centered at the origin, a possible quasielastic contribution depending on the temperature as found by the experiment on IN6, and peaks corresponding to all the possible magnetic transitions.

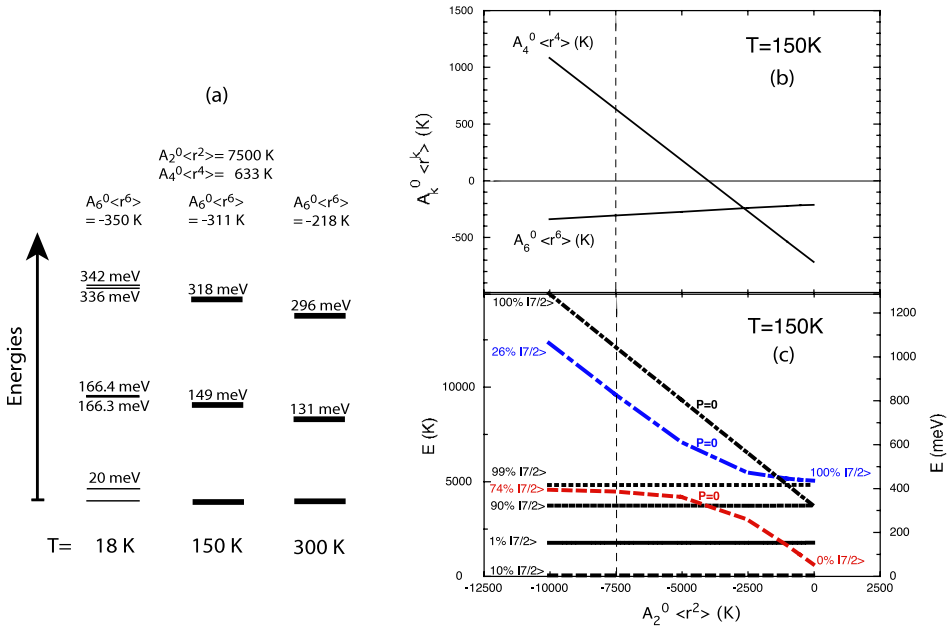

Figure 9. (a) Lowest energy levels calculated with our proposed CEF parameters at 18, 150 and 300 K. (b) Values of $A_4^0\langle r^4\rangle$ and $A_6^0\langle r^6\rangle$ as a function of $A_2^0\langle r^2\rangle$ at $T = 150$ K. (c) Corresponding energy level schemes. For each doublet, the percentage of the $J' = 7/2$ multiplet in the wavefunction is given. For three doublets, transitions from the ground state are forbidden (transition probability $P = 0$).

As the position of the CEF peak is temperature dependent, the four CEF parameters have been first determined using the spectrum at 18 K, the ferromagnetic form factor and the low temperature magnetization curves within and perpendicular to the *c*-plane. The term $A_6^6\langle r^6\rangle$ was found to have no influence and was fixed to zero. The other three parameters are in fact strongly correlated (see below). $A_2^0\langle r^2\rangle$ has to be negative for an easy magnetization lying in the basal plane. One proposed solution is, for $A_2^0\langle r^2\rangle$ fixed at -7500 K, $A_4^0\langle r^4\rangle = 633(\pm 6)$ K and $A_6^0\langle r^6\rangle = -350(\pm 4)$ K. The total calculated spectrum is drawn in the top part of figure 3. The associated level scheme, the lowest levels of which are shown in figure 9(a), indicates that the first excited doublet lies at 166 meV, giving rise to the observed energy transfer. This doublet is split by less than 0.1 meV by the presence of the exchange field at this temperature, and the observed peak then corresponds to two transitions from the ground level, with the same energy. The ground doublet is split by 20 meV, which involves a broadening of the calculated curve close to the elastic peak. If such an excitation presents a dispersion with κ, which is quite likely according to the strongly anisotropic behavior of $CeRh_3B_2$, it is not taken into account in our mean field Hamiltonian and cannot be detected on powders. This explains the discrepancy for $T = 18$ K between calculated and experimental points at low energy transfers.

As the temperature is increased, the position of the CEF peak is shifted towards lower energy transfers. The change between 18 and 150 K could be attributed to the role of the exchange interaction on the splitting in the ferromagnetic state. However, the calculated corresponding change would be 10 meV while the observed one is larger (17 meV). Furthermore, in the paramagnetic state the position of the CEF peak keeps shifting to lower energies when the temperature is increased: between 150 and 300 K it has shifted by 18 meV, which can be explained only by a change in the CEF parameters. As the CEF depends strongly

on the relative lattice parameters of the structure, these changes must be connected with the quite abnormal thermal dependence of the lattice parameters, especially between 100 and 300 K [5]. As the lattice parameters of $CeRh_3B_2$ approach normal values with increasing temperature, its behavior should also become more normal. In normal Ce compounds, where one considers only the $J = 5/2$ ground multiplet, the contribution from the sixth order terms is zero. We thus assumed that only the sixth order parameter $A_6^0\langle r^6\rangle$ was varying. Simultaneous refinements on the spectra for $E_i = 450$ meV at 150 and 300 K and on the magnetic form factor at $T = 150$ K lead to $A_6^0\langle r^6\rangle = -311(\pm 3)$ K at 150 K and $A_6^0\langle r^6\rangle = -218(\pm 4)$ at 300 K. The decrease of $A_6^0\langle r^6\rangle$ as temperature is increased bears out our assumption that $CeRh_3B_2$ tends to a more normal behavior. The HWHMs of all the calculated peaks are given in table 1. The spectra calculated at 150 and 300 K with these new values of $A_6^0\langle r^6\rangle$ are drawn in figure 3 for $E_i = 450$ meV (top) and $E_i = 300$ meV (bottom) and in figure 4 (bottom) for $E_i = 900$ meV.

The correlation between the $A_k^0\langle r^k\rangle$ parameters is shown in figure 9(b), and to any value of $A_2^0\langle r^2\rangle$ down to $-10\,000$ K there corresponds a set of parameters $A_4^0\langle r^4\rangle$ and $A_6^0\langle r^6\rangle$ leading to the same wavefunction of the ground state. The dependence on $A_2^0\langle r^2\rangle$ of the CEF level scheme at $T = 150$ K is drawn in figure 9(c) and the percentage of the $J' = 7/2$ multiplet in the wavefunction of each doublet is also given. One notices that, besides the ground one, three doublets do not depend on the value of $A_2^0\langle r^2\rangle$ (and associated values of $A_4^0\langle r^4\rangle$ and $A_6^0\langle r^6\rangle$), either in their energy or in their wavefunction. The three other doublets are $A_2^0\langle r^2\rangle$ dependent but transitions from the ground state are forbidden (transition probability $\equiv 0$). These features confirm the impossibility to choose a value for $A_2^0\langle r^2\rangle$ and we therefore cannot know the exact CEF total splitting. However, in the energy range reached in our experiments, the splitting of the levels and the transition probabilities are unchanged. A third doublet is located around 320 meV, but as can be seen from the calculated curves in figures 2 and 4 (bottom part) its intensity is very small. In fact, the data points do not show a definite peak around that energy but rather a tail or a level of roughly constant intensity resembling a broad hump or a peak with a much larger width. We note that the intrinsic width (38 meV) of the peak at 150 meV is itself significantly large, for reasons that we do not fully understand at present. Hence, the presence of an even broader peak at higher energies, much broader than suggested by our calculations, cannot be entirely excluded. Such unexplained broadening of CEF excitations at high energies has also been reported [15]. As suggested by the author, some strong relaxation process in the excited level may originate from the coupling to the conduction band. Indeed, strong hybridization effects play an important role in the properties of $CeRh_3B_2$. Clearly, further theoretical input is needed to understand the interesting physical characteristics of this compound.

At all temperatures, a small peak has been observed around 50 meV, which is not predicted by our calculations of the CEF splitting, and its origin remains unclear. One cannot exclude a change in the phonons because of the abnormal variation of the lattice parameters between 100 and 300 K. Moreover, in the ferromagnetic state magnons related to the exchange interactions should also appear, but because of the highly anisotropic character of the magnetic properties of this compound these excitations are expected to be very anisotropic and hence best studied on a single crystal.

4. Conclusion

In conclusion, the present inelastic neutron scattering measurements have confirmed the expected very large crystal electric field effects in $CeRh_3B_2$. Because of the huge splitting of the Ce energy levels, only one well defined CEF peak has been well observed, the position of which is temperature dependent. Using simultaneously other CEF sensitive data, especially

the magnetic form factor and the magnetization data on a single crystal, we have been able to determine the CEF splitting for the lowest levels. Calculations including the two $J = 5/2$ and $J' = 7/2$ multiplets of cerium can explain well the observed spectra as well as the other magnetic results as previously reported.

Appendix. Magnetic inelastic structure factor for multiplets J and J'

According to Balcar and Lovesey [16], the inelastic scattering cross section for transitions between multiplets J and J' can be expressed as a function of the inelastic structure factor $\mathcal{G}(\kappa, J, J')$ as

$$\frac{\mathrm{d}^2\sigma}{\mathrm{d}\Omega \mathrm{d}E'} = r_0^2 \frac{k_f}{k_\mathrm{i}} \mathcal{G}(\kappa, J, J')\delta(\hbar\omega - \Delta\mathrm{E}) \tag{A.1}$$

with

$$r_0 = \frac{\gamma e^2}{mc^2}, \qquad \kappa = \boldsymbol{k} - \boldsymbol{k}'$$

and

$$\mathcal{G}(\kappa, J, J') = \sum_{K'} \frac{3}{K'+1}[A_{J,J'}(K'-1, K') + B_{J,J'}(K'-1, K')]^2 + \sum_{K} \frac{3}{2K+1}[B_{J,J'}(K, K)]^2 \tag{A.2}$$

$A_{J,J'}(K, K')$ and $B_{J,J'}(K, K')$ are orbital and spin contributions to the structure factor, which are linear combinations of the radial integrals $\langle j_K(\kappa)\rangle$. For Ce, $K = 0, 2, 4, 6$ and $K' = 1, 3, 5, 7$.

It turns out that, for given J and J', $\mathcal{G}(\kappa, J, J')$ can be written as a sum of products $\langle j_{K_\mathrm{i}}(\kappa)\rangle\langle j_{K_j}(\kappa)\rangle$:

$$\mathcal{G}(\kappa, J, J') = \sum_{K_\mathrm{i}, K_j} C_{J,J'}(K_\mathrm{i}, K_j) \cdot \left\langle j_{K_\mathrm{i}}(\kappa)\right\rangle\left\langle j_{K_j}(\kappa)\right\rangle. \tag{A.3}$$

The values of the coefficients $C_{J,J'}(K_\mathrm{i}, K_j)$ are tabulated in appendix E.3 of [16] for $J = 5/2$, $J' = J + 1 = 7/2$ (Ce case) and for $J = 7/2$, $J' = J - 1 = 5/2$ (Yb case).

According to the fact that for $J' = J$ the value of $\mathcal{G}(\kappa)$ in the dipole approximation is $\frac{1}{6}J(J+1)g_J^2F^2(\kappa)$ with $F(0) = 1$, $F^2(\kappa, J, J')$ has been deduced from $\mathcal{G}(\kappa, J, J')$ by the relation

$$\mathcal{G}(\kappa, J, J') = \tfrac{1}{6}\mu_\mathrm{eff}(J)\mu_\mathrm{eff}(J')F^2(\kappa, J, J') \tag{A.4}$$

with $\mu_\mathrm{eff}(J) = g_J\sqrt{J(J+1)}$.

References

[1] Dhar S K, Malik S K and Vijayaraghavan R 1981 *J. Phys. C: Solid State Phys.* **14** L321
[2] Kasaya M, Okabe A, Takahashi T, Satoh T, Kasuya T and Fujimori A 1988 *J. Magn. Magn. Mater.* **76–77** 347
[3] Galatanu A, Yamamoto E, Okubo T, Yamada M, Thamizhavel A, Takeuchi T, Sugiyama K, Inada Y and Ōnuki Y 2003 *J. Phys.: Condens. Matter* **15** S2187
[4] Givord F, Boucherle J-X, Galéra R-M, Fillion G and Lejay P 2007 *J. Phys.: Condens. Matter* **19** 356208
[5] Langen J, Jackel G, Schlabitz W, Veit M and Wohlleben D 1987 *Solid State Commun.* **64** 169
[6] Malik S K, Umarji A M, Shenoy G K, Montano P A and Reeves M E 1985 *Phys. Rev.* B **31** 4728

[7] Yamaguchi K, Namatame H, Fujimori A, Koide T, Shidara T, Nakamura M, Misu A, Fukutani H, Yuri M, Kasaya M, Suzuki H and Kasuya T 1995 *Phys. Rev.* B **51** 13952
[8] Alonso J A, Boucherle J-X, Givord F, Schweizer J, Gillon B and Lejay P 1998 *J. Magn. Magn. Mater.* **177–181** 1048
[9] Givord F, Boucherle J-X, Lelièvre-Berna E and Lejay P 2004 *J. Phys.: Condens. Matter* **16** 1211
[10] Martin W C, Zalubas R and Hagan L 1978 Atomic energy levels-the rare earth elements *National Bureau of Standarts Report* NSRDS-NBS 60
Osborn R, Lovesey S W, Taylor A D and Balcar E 1991 *Handbook on the Physics and Chemistry of Rare Earth* vol 14 (Amsterdam: Elsevier)
[11] Boucherle J-X and Schweizer J 1985 *Physica* B **130** 337
[12] Elliott J P, Judd B R and Runciman W A 1957 *Proc. R. Soc.* A **240** 509
[13] Racah G 1943 *Phys. Rev.* **63** 367
[14] Weber M J and Bierig R W 1964 *Phys. Rev.* **134** A1492
[15] Loewenhaupt M 1985 *Physica* B **130** 347
[16] Balcar E and Lovesey S W 1989 *Theory of Magnetic Neutron and Photon Scattering* (Oxford: Clarendon)